Aerosol optical depth enhancement in partly cloudy conditions

D. Chand[1*], R. Wood[2], S. Ghan[1], M. Wang[1], M. Ovchinnikov[1], P. Rasch[1],

S. Miller[3], B. Schichtel[4], T. Moore[5]

1. Atmospheric Science and Global Change Division, Pacific Northwest National Laboratory, Richland, WA 99352

2. Department of Atmospheric Science, University of Washington, Seattle, WA 98095

3. Colorado State University, Cooperative Institute for Research in the Atmosphere, Fort Collins, CO 80523

4. Air Resources Division, National Park Service Fort Collins, CO 80523

5. Western Regional Air Partnership, Western Governors' Association, Fort Collins, CO 80523

* Corresponding author (Duli.Chand@pnnl.gov)

Version 3.0 (Mar 26, 2012)

Abstract

Remote sensing observations of aerosol from surface and satellite instruments are extensively used for atmospheric and climate research. From passive sensors, the apparent cloud-free atmosphere in the vicinity of clouds is affected by undetectable weak signatures of clouds and humidified aerosol to an extent that is poorly known. The mechanisms, e.g., contamination, hygroscopicity, and meteorology controlling the increase in aerosol optical depth ($\Delta\tau$) near clouds have been debated in recent literature. Here we used 11 years of daily global observations at 10x10 km^2 resolution from the Moderate Resolution Imaging Spectrometer (MODIS) on the NASA Terra satellite to quantify τ as a function of cloud cover. Our analysis reveals that, averaged over the globe, the clear sky $\Delta\tau$ (0.05) is enhanced by 25% in the presence of cloudy conditions (cloud fraction of 0.8-0.9 derived from 0.5x0.5 km^2 pixels) compared with relatively clear conditions (cloud fraction of 0.1-0.2). The absolute magnitude of the enhancement in τ is as high as 0.24 near the aerosol source regions and is seasonally variable with maximum in local spring of the Northern and Southern Hemisphere. Unlike the absolute $\Delta\tau$ enhancement, the relative increase in τ is rather consistent in all seasons and is 25-35% in the subtropics and 15-25% at mid and higher latitudes. We use a simple Gaussian pdf model to connect cloud cover and the distribution of relative humidity and use this to argue that much of the enhancement is consistent with aerosol hygroscopic growth in the humid environment surrounding clouds. Consideration of these cloud-dependent τ effects will facilitate understanding aerosol-cloud interactions and reduce the uncertainty in estimates of aerosol radiative forcing by global climate models.

Introduction

The indirect effects of aerosol on clouds are among the most important yet least understood processes associated with climate change. Satellite observations suggest that complex interactions occur between coexisting cloud and aerosol layers [Tanré et al., 1997; Ignatov et al., 2005; Kaufman et al., 2005; Loeb and Manalo-Smith, 2005; Matheson et al., 2005; Loeb and Schuster, 2008]. Observations of aerosol optical depth (AOD or τ) from different satellites have been used for model evaluation and for examining aerosol effects on air quality and climate [Al-Saadi et al., 2005, Quaas et al., 2006, Remer et al., 2006, Chand et al., 2009, Christopher et al., 2010]. Among the contemporary satellite observing systems, the Moderate-Resolution Imaging Spectroradiometers (MODIS) on the National Aeronautics and Space Administration (NASA) Terra and Aqua spacecraft provide perhaps the most comprehensive multispectral record of τ and clouds. One of the primary objectives of MODIS is to provide observation on global aerosol for assessment of its impact on Earth's radiation budget and its role in climate change. MODIS records aerosol data at 10x10 km^2 resolution, which is further aggregated to provide gridded global data products at 1^ox1^o resolution [Remer et al., 2006]. Remer et al. [2005] provided global validation that MODIS is comparable to ground-based AERONET observations over both land and oceans.

Solar reflectance is the principal measurement for satellite-based retrievals of aerosol optical properties over land and oceans. The presence of strongly reflecting clouds represents a major challenge for resolving the relatively weak reflective signals of the more tenuous aerosol layers [Ackerman et al., 1998, Martins et al., 2002]. To overcome these limitations, the MODIS τ retrieval considers only cloud-free pixels; using a sophisticated cloud screen as a preprocessing step (Ackerman et al., 1998). Though great attempts are made to retrieve aerosol properties only from the clear sky pixels in partially cloudy conditions, the effect of the clouds over these clear sky pixels is intangible and may significantly influence the aerosol estimates in several ways. The cloud influence on aerosol retrievals can be due to uptake of water vapor at various stages and scales (Feingold and Morley 2003; McComiskey and Feingold, 2012), decayed or evaporated clouds, so called 'hesitant clouds'—pockets of high humidity that oscillate near saturation (Koren *et al.,* 2009), cloud microphysical process like secondary particle production, and three-dimensional cloud scattering effects (Kaufman et al., 2005; Zhang et al., 2005; Remer et 2006; Mauger and Norris, 2007; Loeb et al.,, 2008; Christopher et al., 2010). Kaufman et al.

(2005) used MODIS and AERONET observations to estimate an enhancement of 0.025 in τ in the vicinity of cirrus and water clouds compared with that far away from clouds at 550 nm. In another similar study, Zhang et al., [2005] estimated that clouds increase τ by 10–20%. In two separate studies, Loeb and Schuster [2008] and Mauger and Norris [2007] pointed to the importance of meteorology (humidity and wind speed) in controlling the τ. Várnai and Marshak [2009, 2011] found that brightness of clear sky systematically increases near clouds and that partial clouds are surrounded by a clear sky transition zone of rapidly changing aerosol optical properties and particle size. In a LIDAR study Tackett and Di Girolamo [2009] showed that aerosol properties such as backscatter and color ratio are enhanced adjacent to cloud edge as far as 3 km, particularly near cloud top and cloud base. Twohy et al [2009] demonstrated the effect of changes in relative humidity on aerosol as far as 20 km from clouds. In as similar study Bar-Or et al. [2010] found the increase in aerosol optical depth as far as 30 km from the transition zone. While most of these studies demonstrate τ enhancements in partly cloudy conditions, none of these studies have explored the effects at large spatial and temporal scales to attempt to understand the large scale behavior of the enhancement. In this study we investigate absolute and relative increase in τ in presence of clouds using satellite observations and model simulations. We begin with a summary of observations and methods, followed by presentation of results and conclusions.

Observations and Methods

We used aerosol optical depth (τ or AOD) and total cloud fraction (CF) observations from MODIS Terra satellite using MOD04_L2 051-version data collection. Daily global aerosol optical depth observations at 10x10 km^2 resolutions are analyzed for the period 2000-2010. These data are valid for about 10:30 a.m. local time. The cloud fraction in aerosol pixels (10x10 km^2) is estimated from high resolution (500x500m) sub-pixels (Remer et al., 2005; Levy et al., 2009). The quality assurance flags are used to select and screen data. As retrievals over water are better than land (Remer et al., 2005), we choose our analysis only over the oceanic regions. The retrieval of aerosol is limited over higher latitudes (>70N and >70S) due to low sunlight and reflective snow covered surfaces, so most of the MODIS aerosol observations used here are available below these latitudes. The τ retrievals are grouped by the CF of each 10x10 km^2 pixel, and we primarily focus on the differences between the mean τ values for 0.8< CF<0.9 and

0.1<CF<0.2, here termed $\tau_{CF.85}$ and $\tau_{CF.15}$ respectively. The absolute enhancement in aerosol optical depth is defined as $\Delta\tau = \tau_{CF.85} - \tau_{CF.15}$. A normalized, or relative, increase in aerosol optical depth is defined as ε ($\varepsilon = \Delta\tau/\tau_{CF.15}$) and both Δτ and ε are gridded to produce near-global maps at 2.5°x2.5° resolution for four seasons. Eleven years of daily data are used to obtain robust statistics.

We also used a Gaussian probability distribution function (pdf) approach to estimate the τ enhancement as a function of cloud fraction, assuming that only hygroscopic aerosol growth is important for determining aerosol optical depth enhancement. The physical basis is that the spatial distribution of relative humidity (RH) shifts to higher values in regions with a greater fractional cloud cover, and so the mean RH for clear sky regions between clouds is greater (Fig. 1). This type of approach actually forms the basis for many statistical cloud schemes used in large scale numerical models, and was first introduced by Sommeria and Deardorff (1977) and Mellor (1977). To quantify this, we estimate the hygroscopic enhancement of light scattering for the clear atmospheric columns under the following assumptions:

(a) The relative humidity pdf, $p(RH)$, is Gaussian at all levels with a standard deviation that is constant with height and a mean that increases linearly from an assumed value of 80% at the surface to some specified maximum RH at the top of the marine boundary layer (MBL). No hygroscopic growth is assumed above this level. The choice of 80% for the mean surface RH is in good agreement with observations over much of the global ocean (e.g., Wood and Bretherton 2006).

(b) The cloud fraction is determined as the saturated part of the RH pdf (RH>100%) at all levels (Fig. 1), i.e.,

$$CF = \int_1^\infty p(RH)dRH. \quad [1]$$

It is the column maximum cloud fraction that is important for the projected cloud fraction as seen from space and this is (by construction) always at the top of the MBL.

(c) The relative AOD enhancement ε is a fractional enhancement over that for a dry aerosol. We assume that the dry aerosol optical depth is independent of cloud cover in a given region. The scavenging might violate this assumption, however here we are trying to establish how much the humidity effect alone might contribute. The enhancement is estimated as a function of height using the clear sky part (RH<100%) of the RH pdf, i.e.,

$$\varepsilon = \int_0^1 p(RH) f(RH) dRH, \quad [2]$$

where $f(RH)$ is the hygroscopic growth factor for aerosol extinction. We then average ε over height to get a column AOD enhancement. We take $f(RH)$ appropriate for sulfate aerosol from Kiehl et al (2000). The growth factor for sea-salt is somewhat higher, but those for pollution aerosol are generally somewhat lower, so our choice represents a compromise but maintains simplicity. For any assumed form of $p(RH)$, there is a parametric relationship between ε and CF through Eqns. [1] and [2]. This relationship is a function of the assumed form of $p(RH)$ and the assumed mean surface RH. The assumptions that $p(RH)$ is Gaussian with a fixed standard deviation, and that the mean surface RH is fixed, results in a unique relationship between ε and CF that depends only upon the assumed pdf width. The pdf width is scale dependent and in general is not well known. However, Wood et al (2002) compiled aircraft estimates of the standard deviation of humidity in the environment of low clouds as a function of length scale. These results suggest that the standard deviation of RH (σ_{RH}) is typically in the range 2-5% (0.02-0.05) at the 10 km scale for marine boundary layer cloud environments. To compare with the MODIS aerosol optical depth observations, we determine the difference in τ between CF=0.85 and that for CF=0.15.

Results and Discussion

Figure 2 shows the seasonal variation in absolute aerosol optical depth enhancement, Δτ, estimated from the MODIS L2 data. Large enhancement is observed near the source regions and over the spring seasons of both hemispheres. A larger enhancement in AOD is observed in NH spring (MAM) then the SH spring (SON). The global median increase in Δτ is about 0.044, and maximum is 0.24 over the oceans near the aerosol source regions over Africa and Asia (Table 1). The large spatial variation in τ unlikely explained by change in cloud fraction since we used the clear sky pixels from partially cloud conditions by selecting samples of two narrow cloud cover ranges. Low levels of Δτ are observed near the inter-tropical convergence zone (ITCZ) and mid-latitudes. The higher Δτ near source regions, and the spatial distribution and gradients in Δτ at global scale indicate that the enhancement is likely due to some inherent property of aerosol, like hygoscopicity or burden of hygroscopic aerosol in vicinity of clouds. We postulate that the effect of clouds adjacent to the satellite field of view humidifies the aerosol in clear sky twilight zone,

and this humidification increases with cloud fraction within the 10x10 km2 pixel. In other words, as the cloud fraction increases within the scene, the potential for clear sky AOD enhancement in proximity of the broken clouds increases in MODIS aerosol products in over each pixel.

This enhancement, $\Delta\tau$, is factor of three higher than the Kaufman et al (2005) estimated AOD enhancement (0.015) as a result of contamination from cirrus clouds, and is a factor of two higher when accounting for cirrus contamination and aerosol growth together. Though Kaufman et al (2005) indicated that cirrus contamination plays a bigger role than hygroscopic growth, the large enhancement in AOD near source regions and lower enhancement over the ITCZ in our analysis indicate a bigger role by hygroscopicity, which we will discuss in more detail in the following sections.

Variations in ε are much less seasonal that those in $\Delta\tau$, (Fig 3), are approximately zonally symmetric and are not strongly dependent upon longitude (Fig.4). For any given season, ε maximizes at the subtropical latitudes (15-35°), where mean values are 0.25-0.35 are common (Fig. 4). Decreases in ε are observed towards the mid-latitudes where mean values are 0.15-0.25 (Fig. 4). Unlike the absolute enhancement $\Delta\tau$ as shown in figure 2, the relative enhancements ε do not depend strongly upon the absolute aerosol loading. In a very few locations, particularly tropical locations in the ITCZ with strong precipitation, ε is observed to be negative. We suspect that this may result from scavenging of the aerosol from frequent convective precipitation. However, regions with negative ε constitute less than 2% of the ocean area. Thus, the presence of clouds enhances the aerosol optical depth most of the ocean.

We note that the subtropical latitudes where ε is greatest contain very limited amounts of high cloud. Over the oceans, much of the aerosol is located at low levels and particularly within the marine boundary layer. In the aerosol product used in this study it is not possible to distinguish between high and low clouds, and so we cannot separate our analysis by cloud type. We might expect hygroscopic growth of aerosol to be largely confined to the clouds in the marine boundary layer where the aerosol primarily resides. Is seems reasonable to suggest that in regions containing high clouds the aerosol would largely be at a different level from the location of the clouds, and would therefore not be strongly enhanced by hygroscopic growth. Thus, regions containing a large fraction of high clouds might be reducing the strength of true enhancements due to hygroscopic growth because these data are necessarily included in our analysis.

Figure 5 shows hygroscopic enhancement of clear sky aerosol optical depth based on the Gaussian pdf model; and the enhancement from MODIS observations is also shown for inter-comparison purpose. We show this as a function of upper value of cloud fraction used to determine ε, i.e., $\varepsilon_{CF} = (\tau_{CF} - \tau_{CF.15})/\tau_{CF.15}$. The curves represent different plausible values of the free parameters, which are the standard deviation of the Gaussian RH pdf and the mean surface RH. Interestingly, the enhancements are in the range 0.15-0.35. The Gaussian values at a cloud fraction of 0.85 are of a similar magnitude to observed enhancements shown in Figures 3 and 4. As discussed above, we do not expect to see enhancements for aerosol within clear sky regions between high clouds. Because cloud height information is not provided in the Level 2 aerosol data used here, we weight the model enhancements by 1-CF_{high} where CF_{high} is the non-liquid cloud cover taken from MODIS Level 3 cloud products, and plot these as a function of latitude (Fig. 6). The weighted model enhancements are now in good agreement with observed latitudinal variability suggesting that the pattern of τ enhancement globally is broadly consistent with aerosol hygroscopic growth. Assuming an average global oceanic CF of 0.51, the estimated global ε is 0.09.

Of course, the agreement between the simple Gaussian hygroscopic growth model and the observations does not definitively prove that hygroscopic growth is the dominant reason for the observed aerosol enhancement near clouds. Though the pdf model captures key aspects of the spatial pattern in ε, the observed zonal mean values are somewhat higher, possibly due to additional effects like 3D light scattering effects (Várnai and Marshak, 2009) and possible meteorological correlations between aerosol and clouds (Matheson et al., 2006, George and Wood 2010). The hygroscopic growth model cannot explain the very lowest values observed in the ITCZ and in the midlatitude storm tracks. Cloud masking by high clouds in these regions, although significant, only reduces the weighted model ε values by 0.12. So scavenging effects in cloudy regions are likely to play some (as yet unknown) role in the global distribution of ε. However, the results are consistent with a GCM model study (Quaas et al., 2010) that found aerosol hygroscopic growth to be the dominant factor controlling the global relationship between cloud cover and aerosol optical thickness.

The explored absolute and relative enhancements in τ at large spatial and temporal scales can be useful to understand the large scale behavior of the clouds on aerosol and the impact of clouds on the aerosol direct radiative forcing. These findings suggesting that while the monthly

and seasonal averaged cloud fraction over the oceanic regions exceeds 50% and may reach as high as 88% [Bar-Or et al., 2010], the large enhancement in aerosol optical depth in presence of clouds need more attention, from complex models like MMF, CAM5 and other global models. Examining enhancements at the regional spatial scale and seasonal timescale should help accurately quantification of the aerosol direct radiative forcing.

Conclusions

Eleven years of daily MODIS observations along with model simulations are used to estimate the enhancement in τ in clear sky zones under partially cloudy conditions at global scale. The summary of results is as follow:

(1) The enhancement of aerosol optical depth as cloud cover increases is quantitatively consistent with hygroscopic growth in humid regions in the vicinity of clouds. The absolute enhancement $\Delta\tau$ (0.044) is about 25% of the global aerosol optical depth at total cloud fraction of 0.85.

(2) The observed enhancement ε at global mean cloud fraction of 0.51 is about 9%.

(3) The enhancement in τ is higher in the spring season of each hemisphere specifically northern hemispheric spring season.

(4) Unlike $\Delta\tau$, the normalized enhancement ε is independent of source region and ranges from 0.25-0.35 in the subtropics and 0.15-0.25 in the midlatitudes.

(5) The normalized enhancement ε shows latitudinal variations with peak at subtropical latitudes, and has a similar spatial pattern in all seasons. There are some small areas (<2% of globe), e.g., ITCZ, showing negative ε, possibly as a result of scavenging the aerosol by rain.

(6) A simple Gaussian pdf model relating the relative humidity in clear sky regions between clouds to the cloud fraction produces enhancements consistent with observations, suggesting that much of the enhancement can be explained by hygroscopic growth.

Acknowledgments

The MODIS data used in this study were acquired as part of NASA's Earth Science Enterprise. PNNL work was supported by the NASA Interdisciplinary Science Program under grant NNX07AI56G, the U.S. Department of Energy (DOE), Office of Science, Atmospheric System Research program, the DOE Scientific Discovery through Advanced Computing (SciDAC) program, and the DOE Decadal and Regional Climate Prediction using Earth System Models (EaSM) program.

Figure captions:

Figure 1 Idealized relative humidity probability density functions demonstrating the relationship between the spatial distribution of relative humidity (RH) and cloud fraction (CF) as per equations 1 and 2.

Figure 2 Climatology of seasonal enhancement in aerosol optical depth ($\Delta\tau$) from MODIS Terra observations. First letter of each month is used to label the seasons (DJF is for Dec-Jan-Feb). Color bar shows the magnitude of $\Delta\tau$.

Figure 3 Same as figure 1 but the normalized enhancement, ε.

Figure 4 Climatology of enhancement in normalized aerosol optical depth (ε) with latitude. The solid black line (starting from lower side) of box plot are 5, 25, 50, 75 and 95 percentiles. The red line in each box is mean if the ε. The lower panel shows the number of data points (in thousands) for each 10 degree latitudinal bin.

Figure 5 Enhancement in clear sky AOD for varying cloud cover derived from hygroscopic growth of aerosol (Kiehl et al., 2000) for three values of the assumed RH pdf width ($\sigma_{RH} = 0.03$, solid thick; $\sigma_{RH} = 0.02$, dotted; $\sigma_{RH} = 0.05$, dashed) and at values of the assumed mean surface RH (80%) using the statistical model. The symbols are enhancement in AOD with CF from 11 years of MODIS Terra observations for DJF (circle), MAM (square), JJA (diamond), and SON (triangle).

Figure 6 Climatology of enhancement in normalized aerosol optical depth *(ε)* from low level clouds with latitude using statistical model based on equation 1 and 2 and weighted with low level cloud fraction (shown by red shadow). The same normalized enhancement *(ε)* from MODIS observations from Figure 4 are also shown here for inter-comparison purpose. The thick black line, + sign and thin black like are 75^{th}, 50^{th} and 25^{th} percentiles of observed ε, respectively. The shaded red area shows the range of the ε from pdf model.

References

Ackerman, S. A., K. I. Strabala,W. P. Menzel, R. A. Frey, C. C.Moeller, and L. E. Gumley (1998), Discriminating clear sky from clouds with MODIS, J. Geophys. Res., 103, 32,141–32,157, doi:10.1029/1998JD200032.

Al-Saadi, J.; Szykman, J.; Pierce, R.B.; Kittaka, C.; Neil, D.; Chu, D.A.; Remer, L.; Gumley, L.; Prins, E.; Weinstock, L.; Macdonald, C.; Wayland, R.; Dimmick, F.; Fishman, J. Improving National Air Quality Forecasts with Satellite Aerosol Observations; Bull. Am. Meteorol. Soc. 2005, 86, 1249-1261.

Bar-Or, R. Z., I. Koren, and O. Altaratz, 2010: Estimating cloud field coverage using morphological analysis. Environ. Res. Lett., 5 (1), 014 022.

Chand, D., R. Wood, T. L. Anderson, S. K. Satheesh, and R. J. Charlson (2009), Satellite-derived direct radiative effect of aerosol dependent on cloud cover, Nature Geoscience, 2, 181– 184, doi:10.1038/ngeo437.

Christopher S. A. and P. Gupta, Satellite Remote Sensing of Particulate Matter Air Quality: The Cloud-Cover Problem, , J. Air & Waste Manage. Assoc. 60:596–602 DOI:10.3155/1047-3289.60.5.596, 2010.

Feingold G and Morley B 2003 Aerosol hygroscopic properties as measured by lidar and comparison with in situ measurements J. Geophys. Res.-Atmos. 108 4327.

George, R.C., and R. Wood, 2010: Subseasonal variability of low cloud radiative properties over the southeast Pacific Ocean. Atmos. Chem. Phys., 10, 4047-4063, doi:10.5194/acp-10-4047-2010.

Ignatov, A., et al. (2005), Two MODIS aerosol products over ocean on the Terra and Aqua CERES SSF datasets, J. Atmos. Sci., 62, 1008–1031.

Kaufman, Y., et al. (2005), A critical examination of the residual cloud contamination and diurnal sampling effects on MODIS estimates of aerosol over ocean, IEEE Trans. Geosci. Remote Sens., 43, 2886–2897.

Kiehl, J. T., Schneider, T. L., Rasch, P. J., Barth, M. C., and Wong, J.: Radiative forcing due to sulfate aerosol from simulations with the National Center for Atmospheric Research Community Climate Model, Version 3, J. Geophys. Res., 105, 1441–1457, 2000.

Koren I, Oreopoulos L, Feingold G, Remer L A and Altaratz O 2008 How small is a small cloud? Atmos. Chem. Phys. 8 3855–64.

Levy, C, Robert, Lorraine A. Remer, Didier Tanré, S. Mattoo, and Yoram J. Kaufman, ALGORITHM FOR REMOTE SENSING OF TROPOSPHERIC AEROSOL OVER DARK TARGETS FROM MODIS: Collections 005 and 051: Revision 2; Feb 2009.

Loeb, N. G., and G. L. Schuster (2008), An observational study of the relationship between cloud, aerosol and meteorology in broken low-level cloud conditions, J. Geophys. Res., 113, D14214, doi:10.1029/2007JD009763.

Martins, J. V., D. Tanre´, L. Remer, Y. Kaufman, S. Mattoo, and R. Levy (2002), MODIS Cloud screening for remote sensing of aerosol over oceans using spatial variability, Geophys. Res. Lett., 29(12), 8009, doi:10.1029/2001GL013252.

Matheson, M. A., J. A. Coakley Jr., and W. R. Tahnk (2006), Multiyear Advanced Very High Resolution Radiometer observations of summertime stratocumulus collocated with aerosol in the northeastern Atlantic, J. Geophys. Res., 111, D15206, doi:10.1029/2005JD006890.

McComiskey, A. and Feingold, G.: The scale problem in quantifying aerosol indirect effects, Atmos. Chem. Phys., 12, 1031-1049, doi:10.5194/acp-12-1031-2012, 2012.

Mellor, G. L., 1977: The Gaussian cloud model relations. J. Atmos. Sci., 34, 356–358.

Mauger, G. S., and J. R. Norris (2007), Meteorological bias in satellite estimates of aerosol-cloud relationships, Geophys. Res. Lett., 34, L16824, doi:10.1029/2007GL029952.

Quaas, J., Stevens, B., Stier, P., and Lohmann, U.: Interpreting the cloud cover – aerosol optical depth relationship found in satellite data using a general circulation model, Atmos. Chem. Phys., 10, 6129–6135, doi:10.5194/acp-10-6129-2010, 2010.

Remer, L. A., et al. (2005), The MODIS aerosol algorithm, products and validation, J. Atmos. Sci., 62, 947–973, doi:10.1175/JAS3385.1.

Remer, L. A., and Y. J. Kaufman (2006), Aerosol direct radiative effect at the top of the atmosphere over cloud-free ocean derived from four years of MODIS data, Atmos. Chem. Phys., 6, 237– 253.

Sommeria, G., and J. W. Deardorff, 1977: Subgrid-scale condensation in models of nonprecipitating clouds. J. Atmos. Sci., 34, 344–355.

Tackett, J. L., and L. Di Girolamo (2009), Enhanced aerosol backscatter adjacent to tropical trade wind clouds revealed by satellite-based lidar, Geophys. Res. Lett., 36, L14804, doi:10.1029/2009GL039264.

Tanré, D., Y. J. Kaufman, M. Herman, and S. Mattoo, "Remote sensing of aerosol over oceans from EOS-MODIS.," J. Geophys. Res., vol. 102, pp. 16 971–16 988, 1997.

Twohy, C. H., J. A. Coakley Jr., and W. R. Tahnk (2009), Effect of changes in relative humidity on aerosol scattering near clouds, J. Geophys. Res., 114, D05205, doi:10.1029/2008JD010991.

Várnai, T., and A. Marshak (2009), MODIS observations of enhanced clear sky reflectance near clouds, Geophys. Res. Lett., 36, L06807, doi:10.1029/2008GL037089.

Várnai, T. and A. Marshak, Global CALIPSO Observations of Aerosol Changes Near Clouds TamásVárnai and Alexander Marshak, IEEE GEOSCIENCE AND REMOTE SENSING LETTERS, VOL. 8, NO. 1, JANUARY 2011

Wood, R, P. R. Field, and W. R. Cotton, 2002: Autoconversion rate bias in stratiform boundary layer cloud parameterizations. Atmos. Res., 65, 109–128.

Wood, R., and C. S. Bretherton, 2006: On the relationship between stratiform low cloud cover and lower-tropospheric stability. J. Clim., 19, 6425-6432.

Zhang, J., J. S. Reid, and B. N. Holben (2005), An analysis of potential cloud artifacts in MODIS over ocean aerosol optical thickness products, Geophys. Res. Lett., 32, L15803, doi:10.1029/2005GL023254.

Table 1. Seasonal statistics of absolute and relative enhancement in AOD estimated from the observations used in Figures 1 and 2.

Season	**Absolute enhancement, $\Delta\tau$**			**Relative enhancement, ε**		
	25^{th}%	50^{th}%	75^{th}%	25^{th}%	50^{th}%	75^{th}%
DJF	0.035	0.045	0.055	0.18	0.26	0.34
MAM	0.031	0.042	0.057	0.16	0.24	0.32
JJA	0.030	0.040	0.055	0.16	0.25	0.32
SON	0.037	0.047	0.055	0.19	0.26	0.34
Annual	0.033	0.044	0.055	0.17	0.25	0.33

Figure 1

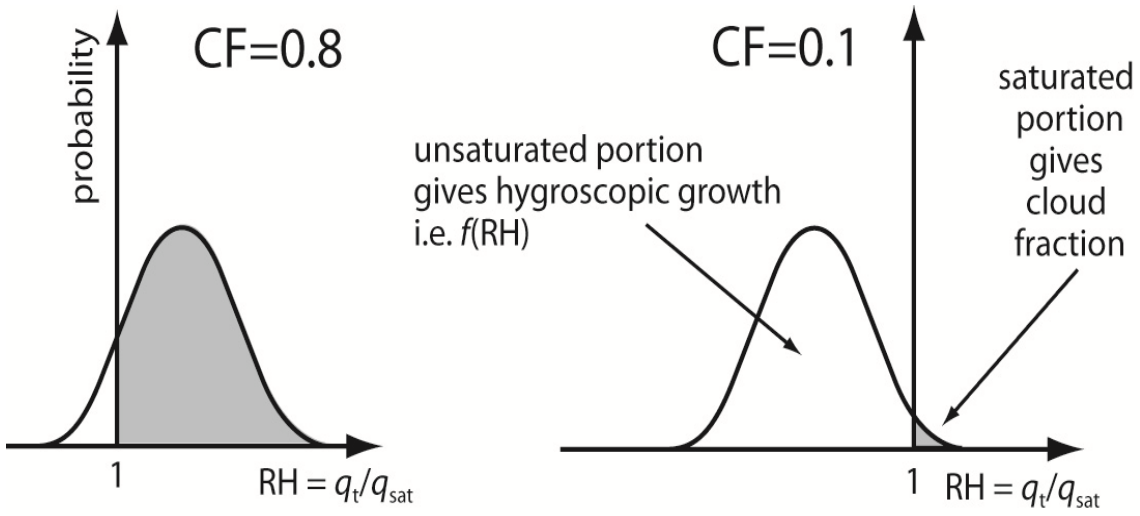
probability
CF=0.8
1
RH = q_t/q_{sat}
CF=0.1
unsaturated portion
gives hygroscopic growth
i.e. *f*(RH)
saturated
portion
gives
cloud
fraction
1
RH = q_t/q_{sat}

Figure 2

.

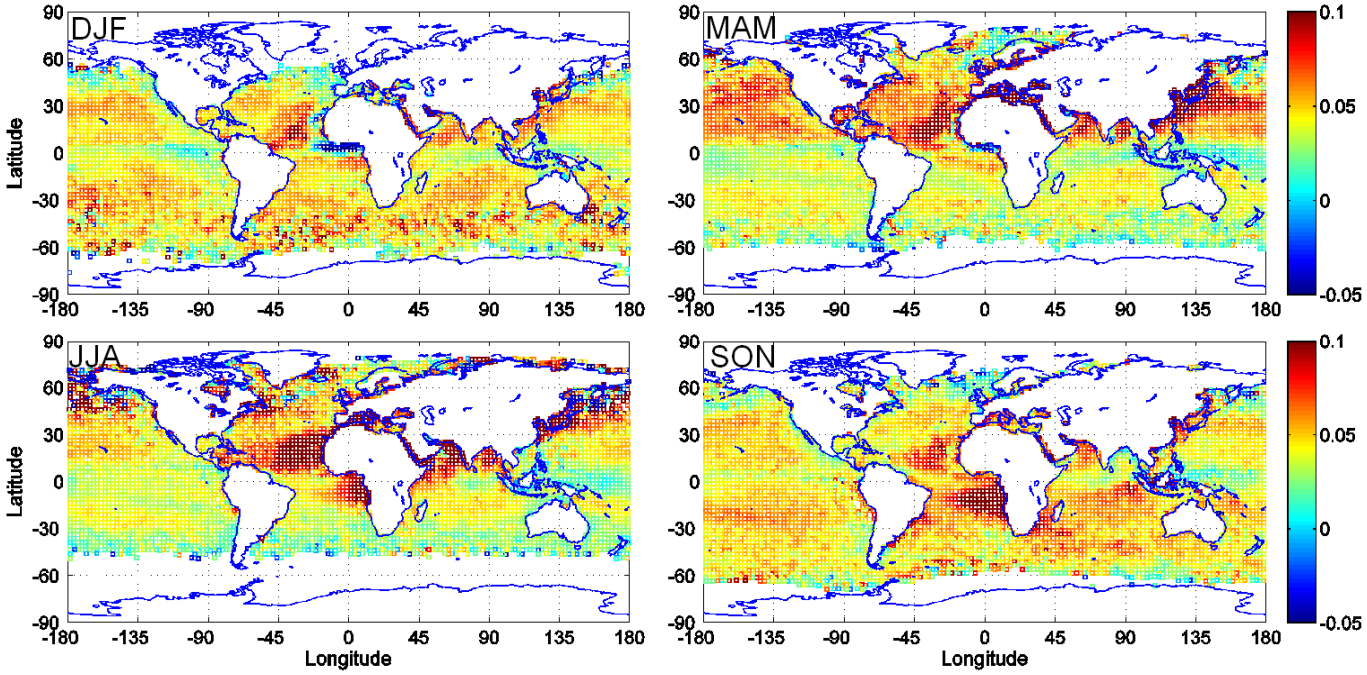
DJF
MAM
JJA
SON
Latitude
Longitude
90
60
30
0
-30
-60
-90
-180
-135
-90
-45
0
45
90
135
180
0.1
0.05
0
-0.05

Figure 3

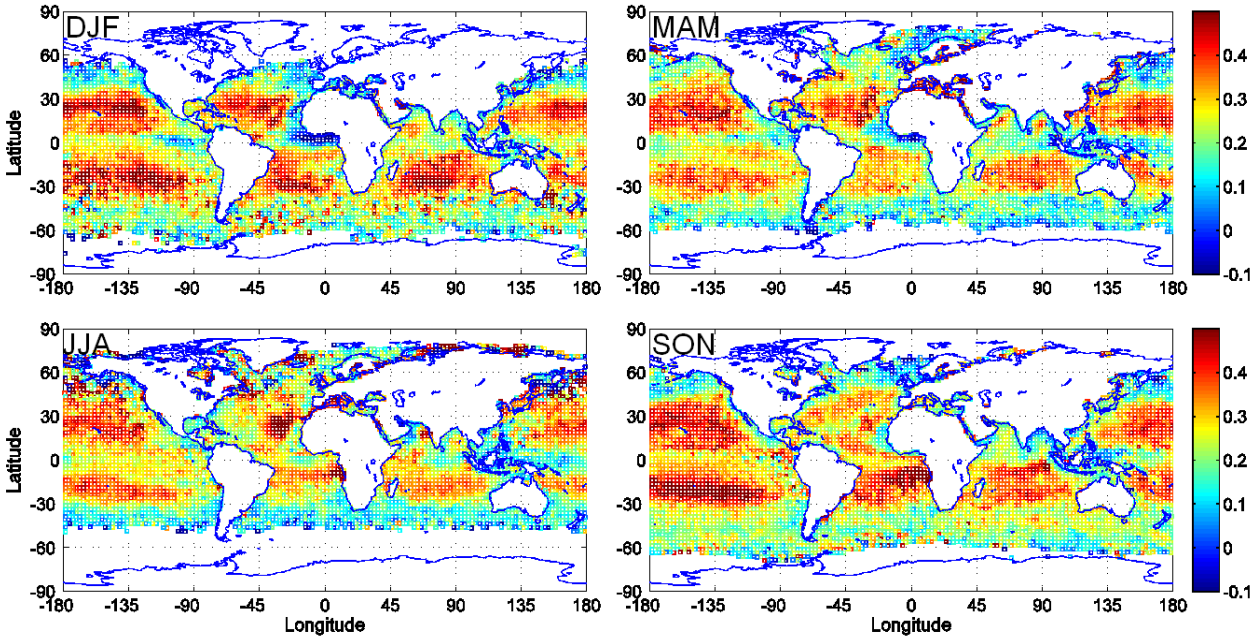
DJF
MAM
JJA
SON
Latitude
Longitude
90
60
30
0
-30
-60
-90
-180
-135
-90
-45
0
45
90
135
180
0.4
0.3
0.2
0.1
0
-0.1

Figure 4

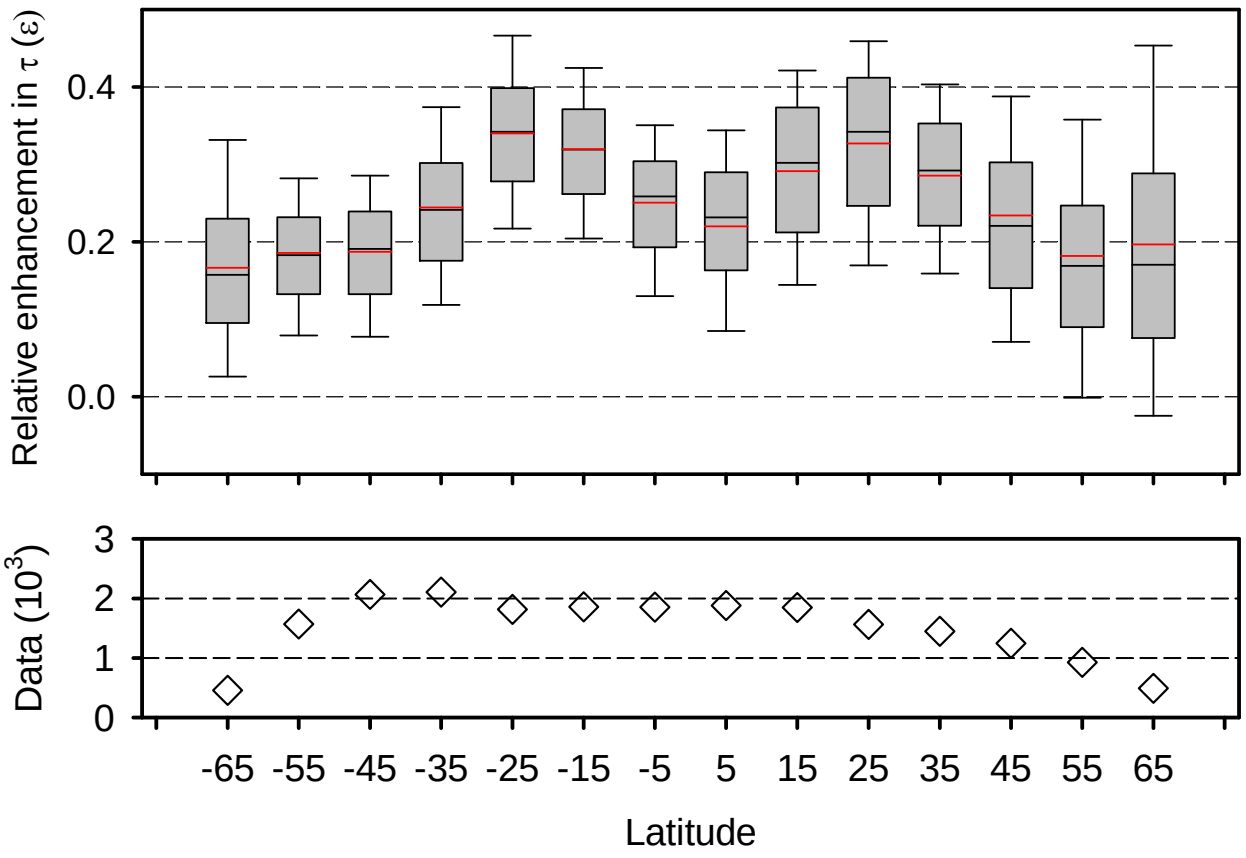
Relative enhancement in τ (ε)
0.4
0.2
0.0
Data (10^3)
3
2
1
0
-65 -55 -45 -35 -25 -15 -5 5 15 25 35 45 55 65
Latitude

Figure 5

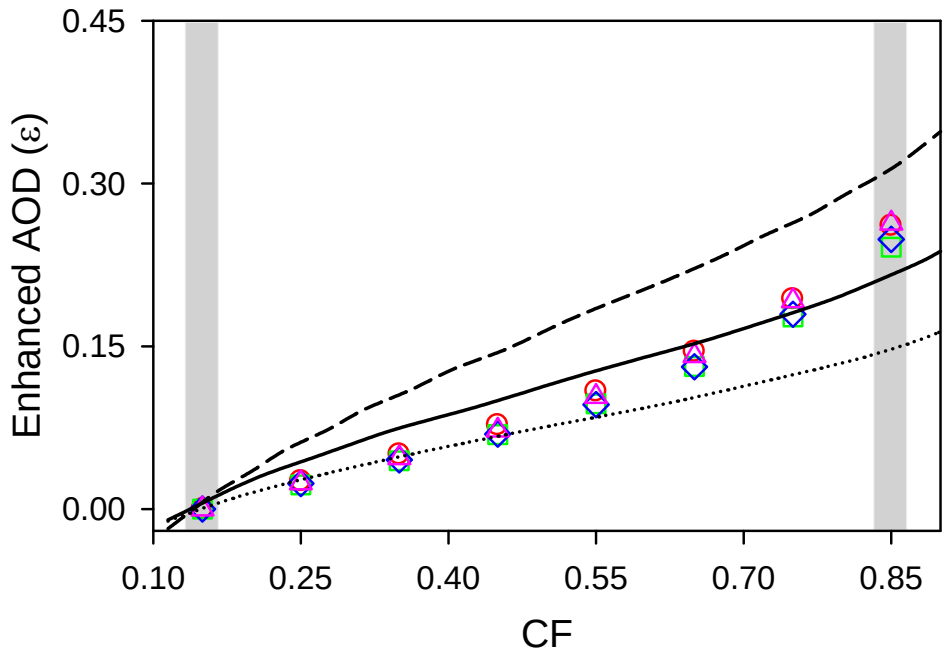

Figure 6: